Numerical simulation of time delays in light-induced ionization

Jing Su, Hongcheng Ni, Andreas Becker, and Agnieszka Jaroń-Becker
JILA and Department of Physics, University of Colorado, Boulder, Colorado 80309-0440, USA
(Received 23 November 2012; published 27 March 2013)

We apply a fundamental definition of time delay, as the difference between the time a particle spends within a finite region of a potential and the time a free particle spends in the same region, to determine results for photoionization of an electron by an extreme ultraviolet laser field using numerical simulations on a grid. Our numerical results are in good agreement with those of the Wigner-Smith time delay, obtained as the derivative of the phase shift of the scattering wave packet with respect to its energy, for the short-range Yukawa potential. In the case of the Coulomb potential we obtain time delays for any finite region, while—as expected—the results do not converge as the size of the region increases towards infinity. The impact of an ultrashort near-infrared probe pulse on the time delay introduced here is analyzed for both the Yukawa and the Coulomb potential and is found to be small for intensities below 10^{13} W/cm^2.

DOI: 10.1103/PhysRevA.87.033420 PACS number(s): 33.80.Rv, 33.80.Wz

I. INTRODUCTION

The development of attosecond extreme ultraviolet (XUV) laser technology in recent years has offered the opportunity to observe and control the dynamics of electrons and the coupling to nuclear dynamics in atoms and molecules on their natural time scale. In particular, the capability to lock XUV pulses to a near-infrared (near-IR) pulse has initiated the development of techniques in which the dynamics is triggered by the attosecond pulse and observed as a function of the delay between the XUV and the near-IR pulses. Experimental observations include, among others, the time resolution of the Auger decay [1], the dynamics of electrons in valence shell [2] and excited states [3,4], shake-up processes [3], and delays in the photoemission of electrons from different bands in a solid [5] or different subshells in an atom [6,7].

In particular, observations of substantial time delays during photoionization of atoms have generated significant theoretical interest (e.g., [6–22]). These measurements are often analyzed in terms of the so-called Wigner-Smith (WS) time delay (e.g., [6–8,10,11,13,18,22]). The WS time delay accounts for the delay in the propagation of a particle in a potential as compared to that of a corresponding free particle towards infinity in space in an atomic or molecular scattering scenario [23,24]. It has been pointed out [24] that this definition leads to a well-defined time delay as long as the potential vanishes quickly enough at large distances. In contrast, for long-range potentials, such as the Coulomb potential, the WS time delay is an intrinsically ill-defined concept. In view of this deficiency of the WS time delay concept, sometimes short- and long-range parts of a potential are considered separately (e.g., [10,11,18]). For a given problem it may, however, be unclear where such a separation is justified. Furthermore, the WS time delay is often calculated via the derivative of the phase shift of the wave function with respect to the energy of the particle (e.g., [8,10,11,13,18,23,24]). This time-independent approach does not enable an analysis of the delay as a function of time during the interaction.

We therefore seek an alternative time-dependent theoretical approach to calculate time delays in photoionization, which addresses some of the concerns regarding the WS time delay and its determination via the phase derivative outlined in the previous paragraph. We further attempt to apply such an approach in time-dependent numerical grid simulations which are known to be a powerful tool in calculating and analyzing processes on an ultrashort time scale. The present theoretical analysis of a time delay is intended to be general and not focused, in particular, on the recent streaking experiments. Once formulated, tested, and established, this may turn out in the future to be a useful step towards understanding the physics of time delays in streaking experiments and other precise measurements of ultrashort time scales.

Our proposal is based on the quantum mechanical expression for the time a particle spends inside a certain region R of a potential. By comparing this time to the corresponding time for a free particle, a time delay is given, which is well-defined for any finite region. This approach is also known to be the basis for the WS time delay itself, which is nothing other than the limit, if it exists, as the region R grows to infinity [23,24]. This fundamental definition of a time delay has not been applied in the analysis of time-dependent processes initiated or driven by ultrashort laser pulses. However, it offers a few interesting features: First, as mentioned above, for any finite region R the time delay is well defined for any physical relevant potential and independent whether or not the limit for an extension of the region towards infinity exists. This enables a theoretical analysis in particular for long-range potentials without any restriction of the potential. Second, in the limit to infinity, if well-defined, the time delay should converge to the WS delay. Third, the time delay can be determined as a function of time after the emission of the photoelectron, in the case of a streaking experiment even during the interaction with the probe pulse. This expands the options for a theoretical analysis of ultrashort time-dependent processes. Fourth, there is no *a priori* separation of short- and long-range parts in the potential necessary and the influence of both contributions can be studied.

In this paper we present and discuss the application of the above-mentioned time-delay concept to the photoionization process. We further show how the concept can be utilized in time-dependent numerical simulations on a grid using the backpropagation technique. While the theoretical approach is developed and formulated in 3D, we restrict ourselves to an implementation in 1D calculations. This is done in

the present proof-of-principle study in order to carefully investigate the convergence of the results with respect to the grid parameters, which appears to be appropriate in view of the required resolution of time delays on the order of a few attoseconds. An application of the approach to more dimensions is straightforward. We also show that in our application of the concept the numerical results indeed agree with the WS time delay, in case the appropriate limit exists. We may emphasize that any time delay determined in the present context is well-defined, even in the case of the Coulomb potential, since we consider delays over finite ranges in space only. Besides the introduction of this complementary concept and the demonstration of its application to photoionization, we consider one aspect of the recent observations of time delays using attosecond XUV pump and near-IR probe pulses, namely the impact of the probe pulse on the time delay introduced here. We may note that this time delay does not necessarily correspond to or fully include the time delay observed in recent streaking experiments, since our method calculates (or measures) the time delay directly in the time domain while, in contrast, in the streaking technique a time delay is determined indirectly via a momentum (or energy) measurement. Since the probe pulse is usually ultrashort, the effect occurs over a finite time and, hence, during the propagation of the electron over a finite distance R in the potential only. Thus, the present concept appears to be well suited and can therefore be used to analyze the impact of the probing pulse for short- as well as long-range potentials.

The paper is organized as follows. We first provide the basic definitions for the calculation of a time delay with and without a strong probing field and discuss the application in numerical simulations. We then show that the numerical results for single XUV photoionization are well-defined over finite distances but clearly do not converge as $R \to \infty$ in the Coulomb case, in agreement with the discussion given in the early work by Smith [24]. On the other hand, our numerical results are in good agreement with those for the original WS time delay in the case of a short-range potential. Finally, we investigate the impact of an ultrashort near-IR probing pulse on the results for the time delay. Our results indicate that the effect is small as long as the intensity of the probe pulse does not exceed 10^{13} W/cm^2.

II. THEORETICAL METHOD

In this section we introduce the theoretical method, which we use to obtain time delays associated with the ionization of a target system in numerical simulations. To this end, we will first provide a set of basic definitions used in the method before we discuss its use in numerical simulations.

A. Basic definitions

For a particle in a given state $\Psi(\boldsymbol{r},t)$ the time spent inside a region R with a potential $V(\boldsymbol{r})$ can be expressed as (Hartree atomic units, $e = m = \hbar = 1$ are used throughout the paper) [25]

$$t_{\Psi,R} = \int_{-\infty}^{\infty} dt \int_R d\boldsymbol{r} |\Psi(\boldsymbol{r},t)|^2. \tag{1}$$

While $t_{\Psi,R}$ is, in general, finite for finite regions and any $\Psi(\boldsymbol{r},t)$, it is useful to compare $t_{\Psi,R}$ to the time spent by the free particle in R (or another reference time):

$$t_{\Psi^{(0)},R} = \int_{-\infty}^{\infty} dt \int_R d\boldsymbol{r} |\Psi^{(0)}(\boldsymbol{r},t)|^2. \tag{2}$$

Here, $\Psi^{(0)}(\boldsymbol{r},t)$ is the free-particle state corresponding to $\Psi(\boldsymbol{r},t)$. The difference between $t_{\Psi,R}$ and $t_{\Psi^{(0)},R}$ defines the time delay associated with $\Psi(\boldsymbol{r},t)$, the region R and the potential $V(\boldsymbol{r})$:

$$\Delta t_{\Psi,R} = t_{\Psi,R} - t_{\Psi^{(0)},R}. \tag{3}$$

The quantity $\Delta t_{\Psi,R}$ is known to have a finite limit as the radius of R grows to infinity if the interaction vanishes quickly enough [24]. Thus, $\Delta t_{\Psi,R\to\infty}$ (and the associated quantum mechanical operator) is well-defined for short-range potentials $V(\boldsymbol{r})$ only. Provided that the limit exists, $\Delta t_{\Psi,R\to\infty}$ can be also expressed as the energy derivative of the phase shift φ induced by the potential $V(\boldsymbol{r})$,

$$\Delta t_{\Psi,R\to\infty} = \Delta t_{\mathrm{WS}} = \frac{d\varphi}{dE}, \tag{4}$$

which is commonly known as the WS time delay.

The definition given above provides a useful concept to calculate time delays in time-dependent processes, in particular on an ultrashort time scale. While it is known as the basis for a derivation of the WS time delay in scattering scenarios, to the best of our knowledge it has not been applied for the theoretical analysis of processes initiated or driven by ultrashort intense laser pulses. As an application, we intend to obtain time delays in the form of the time difference, given in Eq. (3), for a photoionization process. Physically, we are interested in the time that an—initially bound—electron needs to leave a certain region (centered about the location of the residual target) following ionization due to the interaction with an external light field. To this end, we note that the expressions above can be readily applied to a particle in a superposition of states and therefore consider the ionizing part (i.e., the continuum parts) of the wave function $\Psi_i^{(\mathrm{ion})}(\boldsymbol{r},t)$ in our adoption of Eq. (1),

$$t_{\Psi_i,R} = \frac{1}{P_{\mathrm{ion}}} \int_{-\infty}^{\infty} dt \int_R d\boldsymbol{r} \left|\Psi_i^{(\mathrm{ion})}(\boldsymbol{r},t)\right|^2, \tag{5}$$

where $P_{\mathrm{ion}} = \int_{-\infty}^{\infty} d\boldsymbol{r} |\Psi_i^{(\mathrm{ion})}(\boldsymbol{r},t\to\infty)|^2$ is the ionization probability. We renormalize the wave function via division by P_{ion} in Eq. (5) in order to be able to compare times and time delays arising for the ionization from different initial bound states $\Psi_i(\boldsymbol{r},t=0)$. We can then define the time delay associated with the ionization from a specific initial bound state analogous to Eq. (3) as

$$\Delta t_{\Psi_i,R} = t_{\Psi_i,R} - t_{\Psi_i^{(0)},R}, \tag{6}$$

where $\Psi_i^{(0)}(\boldsymbol{r},t)$ is the free-particle state corresponding to the ionizing part of the wave function after transition from the initial state $\Psi_i(\boldsymbol{r},t=0)$. According to this definition we expect negative values for the time delays, since a free wave packet should spend more time in a given region R than the corresponding wave packet that has the same asymptotic energy propagating in an attractive potential. We expect that

$\Delta t_{\Psi_i,R}$ has a well-defined finite limit (for $R \to \infty$), i.e., the WS time delay, for short-range potentials, but not necessarily for long-range potentials such as the Coulomb interaction. In view of the intrinsic negative time delays for finite regions, we expect that the limit value is negative as well. We also consider the difference in the time delays for the ionizations from two different initial states $\Psi_i(\boldsymbol{r},t=0)$ and $\Psi_j(\boldsymbol{r},t=0)$ as

$$\Delta T(\Psi_i,\Psi_j;R) = \Delta t_{\Psi_i,R} - \Delta t_{\Psi_j,R}. \tag{7}$$

B. Numerical simulations of time delays

In order to use the above definitions in a numerical simulation of a photoionization process we need to identify the ionizing part of the wave function $\Psi_i^{(\mathrm{ion})}(\boldsymbol{r},t)$, as well as the corresponding free-particle state $\Psi_i^{(0)}(\boldsymbol{r},t)$. Since it is not straightforward to obtain, e.g., the time of ionization (e.g., [8]) and the form of the wave packet after the transition into the continuum, it appears to be difficult to make use of Eq. (6) in a numerical simulation directly. We circumvent this obstacle by using the backpropagation technique.

We first solve the time-dependent Schrödinger equation (TDSE) of the system, initially in the state $\Psi_i(\boldsymbol{r},t=0)$, under the interaction with the external light field on a space-time grid:

$$i\frac{\partial}{\partial t}\Psi(\boldsymbol{r},t) = \left(\frac{\boldsymbol{p}^2}{2} + V(\boldsymbol{r}) + V_{\mathrm{light}}(t)\right)\Psi(\boldsymbol{r},t), \tag{8}$$

where $\boldsymbol{p}$ is the momentum operator and $V_{\mathrm{light}}(t)$ represents the interaction with the ionizing light field. After the end of the interaction with the light field we separate the ionizing part of the wave function from the remaining bound parts, either via projection onto analytically or numerically known states or via spatial separation of the ionizing part at large distances on the grid. After removal of the bound parts we propagate the remaining ionizing part of the wave function backwards in time without taking account of the interaction with the light field using two different Hamiltonians, once including the potential $V(\boldsymbol{r})$,

$$i\frac{\partial}{\partial t}\Psi_i^{(\mathrm{ion})}(\boldsymbol{r},t) = \left(\frac{\boldsymbol{p}^2}{2} + V(\boldsymbol{r})\right)\Psi_i^{(\mathrm{ion})}(\boldsymbol{r},t), \tag{9}$$

and once as a free particle,

$$i\frac{\partial}{\partial t}\Psi_i^{(0)}(\boldsymbol{r},t) = \frac{\boldsymbol{p}^2}{2}\Psi_i^{(0)}(\boldsymbol{r},t). \tag{10}$$

In order to calculate the time delay $\Delta t_{\Psi_i,R}$ for a given region R, the wave packet has to be located outside of R at the start of the backpropagation and the propagation needs to be terminated as the wave packet reaches the center of R, i.e., the location of the residual target ion. The latter point will be further discussed in the application of the method below.

III. APPLICATION TO SINGLE PHOTOIONIZATION BY AN XUV PULSE

A. Model systems

The theoretical method outlined above is, in general, applicable to ionization of an atom or molecule in any light field. Here we present results for the application to photoionization of an electron initially bound in two different model potentials. First, we used a short-range Yukawa potential in 1D,

$$V_{\mathrm{Y}}(x) = -\frac{Z}{\sqrt{x^2+a}}e^{-\frac{|x|}{b}}, \tag{11}$$

where Z is the effective nuclear charge, a is the soft-core parameter, and b is a parameter that determines the effective range of this 1D potential. For our simulations we chose $Z = 3.0$, $a = 2.0$, and $b = 30.0$, which relate to energies of -1.6742 and -1.0124 a.u. of the ground and first excited states. As a long-range interaction we made use of the Coulomb potential in 1D:

$$V_{\mathrm{C}}(x) = -\frac{Z}{\sqrt{x^2+a}}. \tag{12}$$

For $Z = 3.0$ and $a = 2.0$, the energies of the lowest two states are -1.7117 and -1.0807 a.u., which are close to the energies of the Yukawa potential.

For the interaction with the XUV light pulse we used length gauge, i.e.,

$$V_{\mathrm{light}}(t) = E_{\mathrm{XUV}}(t)x, \tag{13}$$

where E_{XUV} represents a linearly polarized pulse with a $\sin^2$ envelope, i.e.,

$$E_{\mathrm{XUV}}(t) = E_0 \sin^2(\pi t/\tau)\sin(\omega t + \phi), \tag{14}$$

where E_0 is the peak amplitude, τ is the pulse duration, ω is the central frequency, and ϕ is the carrier-envelope phase (CEP).

To solve the corresponding TDSE, we used the common Crank-Nicolson method in a grid representation. In general, we used a spatial step of $\delta x = 0.02$ and a time step of $\delta t = 0.002$ in our simulations. The grid extended from -4000 to 4000 a.u. for the numerical simulations of the model systems interacting with an XUV pulse to hold the full wave function on the grid. The initial ground and first excited states were obtained by imaginary time-propagation method. We continued the propagation of the wave function after the interaction with the XUV pulse until the ionizing parts of the wave packet reached a distance beyond $|x| \geqslant 500$ and hence were well separated from the remaining bound parts. This allowed us to remove the latter parts from the grid and remain the ionizing parts of the wave function only. We then propagated the ionizing parts at negative and positive x backwards in time independently, either under the influence of the potential, V_Y or V_C, or as a free particle. We determined the corresponding times $t_{\Psi_i,R}$ and $t_{\Psi_i^{(0)},R}$ for both parts of the ionizing wave function and added the two contributions. In the 1D calculations we defined the region as $R = [\pm x_{\mathrm{inner}}, \pm x_{\mathrm{outer}}]$, where x_{inner} and $x_{\mathrm{outer}} \leqslant 500$ are the inner and outer boundaries, respectively, and the $\pm$ signs apply to backpropagation of the two parts of the ionizing wave packet along the positive/negative x axis, respectively. We absorbed the wave function beyond the inner boundary x_{inner} using the exterior complex scaling method [26,27].

B. Boundaries and grid parameters

Based on the results of recent observations [6,7] and calculations [8,10–12,22], we expect that the time delay $\Delta t_{\Psi_i,R}$ as well as the difference in the time delays for the ionization

TABLE I. Results of numerical calculations for the times $t_{\Psi_g,R}$, $t_{\Psi_g^{(0)},R}$ and the time delay $\Delta t_{\Psi_g,R}$ for different spatial steps δx and a fixed time step of $\delta t = 0.002$. Results are obtained for ionization from the ground state of the 1D Yukawa potential and $R = [0, \pm 460]$. The parameters of the XUV pulse were peak intensity $I = 1 \times 10^{15}$ W/cm^2, frequency $\omega = 100$ eV, pulse duration $\tau = 400$ as, and CEP $\phi = 0$.

Spatial step	$t_{\Psi_g,R}$	$t_{\Psi_g^{(0)},R}$	$\Delta t_{\Psi_g,R}$
0.5	275.3389	274.4569	0.8820
0.2	240.6028	241.5927	−0.9899
0.1	236.8736	237.9043	−1.0307
0.05	235.9751	237.0109	−1.0358
0.02	235.7258	236.7628	−1.0370
0.01	235.6903	236.7274	−1.0371

from different initial states $\Delta T(\Psi_i, \Psi_j, R)$ are of the orders of a few tens of attoseconds. Resolution of such small times requires an analysis of the time and spatial steps in the numerical simulations in order to establish appropriate limits for grid parameters towards a convergence of the results in the present studies. In Tables I and II we present a set of numerical results obtained for different δx and δt in the case of the Yukawa potential. We see that a convergence of the time delay $\Delta t_{\Psi_i,R}$ within less than 0.001 a.u. (i.e., <0.025 as) is reached for a time step of $\delta t = 0.002$ and a spatial step of $\delta x = 0.02$. Similar conclusions hold for our studies with the Coulomb potential as well.

As mentioned above, the time delay $\Delta t_{\Psi_i,R}$ depends on the size of the region R, and should be negative and converge to a finite limit for short-range potentials only. To test these expectations, we performed a set of simulations for the time delays for photoionization from the ground and excited states of both potentials as a function of the outer boundary x_{outer} by fixing $x_{\text{inner}} = 0$, i.e., for $R = [0, x_{\text{outer}}]$. As expected, the values for the time delays are negative and decrease for an increase of the region R for each of the results presented in Fig. 1. For the Yukawa potential (panel a) convergence is found for outer boundaries $x_{\text{outer}} > 150$. Consequently, for large values of the outer boundary we obtain a well-defined value for the time difference ΔT of the time delays for ionization from the ground and the excited states.

In contrast, our results do not show a convergence for the time delays as a function of the outer boundary in the case of the long-range Coulomb potential [see Fig. 1(b)]. This reflects the well-known logarithmic divergence of the time delay for this kind of potential and, hence, for ionization from any bound state within the potential. Of course, in these cases a WS time delay as the derivative of the phase shift [cf. Eq. (4)] cannot be defined as well, since its derivation requires a finite limit of $\Delta t_{\Psi_i,R\to\infty}$. It is interesting to point out that the results in Fig. 1(b) further show that the logarithmic divergence is, in general, still present for the difference between a pair of time delays obtained for the ionization from two different initial states. Thus, such a time delay difference does not simply depend on the short-range character of the potential but contains information about the long-range part of the potential and is therefore not well-defined as well. The present results agree well with the conclusions of early works on time

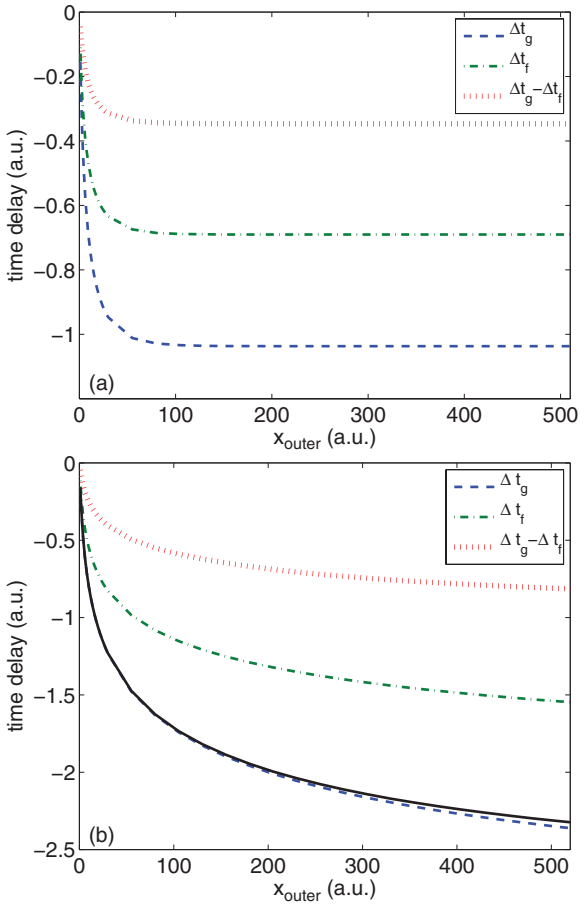

FIG. 1. (Color online) Time delays $\Delta t_{\Psi_i,R}$ and time difference $\Delta T(\Psi_i, \Psi_j, R)$ as a function of the outer integration boundary x_{outer} for two potentials: (a) short-range Yukawa potential and (b) long-range Coulomb potential. Time delays obtained for the ground and first-excited states are represented by blue dashed lines and green dash-dotted lines, respectively, while the red dotted lines show the results for the time difference between the delays. In (b) the black solid and blue dashed lines correspond to two different forward propagation distances: $\langle x_{\text{forward}} \rangle = 2000$ and 3000, respectively, for the ionization from the ground state. In all calculations we have used an XUV pulse with peak intensity $I = 1 \times 10^{15}$ W/cm^2, central frequency $\omega = 100$ eV, pulse duration $\tau = 400$ as, and CEP $\phi = 0$ for the ionization.

TABLE II. Results of numerical calculations for the times $t_{\Psi_g,R}$ and $t_{\Psi_g^{(0)},R}$ and the time delay $\Delta t_{\Psi_g,R}$ for different time steps δt and a fixed spatial step of $\delta x = 0.02$. All the other parameters were the same as in Table I.

Time step	$t_{\Psi_g,R}$	$t_{\Psi_g^{(0)},R}$	$\Delta t_{\Psi_g,R}$
0.1	237.0072	238.0431	−1.0359
0.05	236.0391	237.0757	−1.0366
0.02	235.7752	236.8121	−1.0369
0.01	235.7378	236.7747	−1.0369
0.005	235.7284	236.7654	−1.0370
0.002	235.7258	236.7628	−1.0370
0.001	235.7254	236.7624	−1.0370

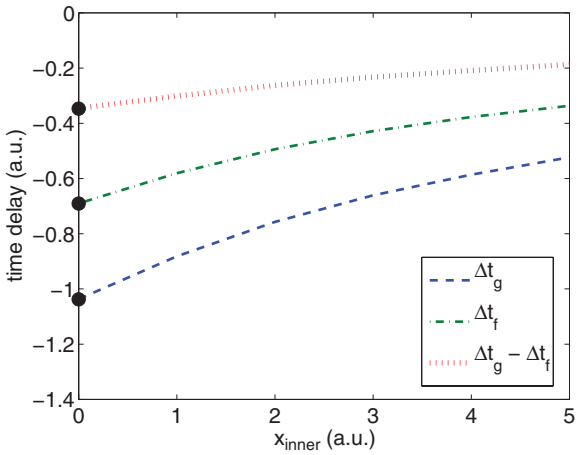

FIG. 2. (Color online) Time delays and difference between time delays as a function of inner integration boundary x_{inner}. Symbols and laser parameters are the same as in Fig. 1. We also plotted the WS time delays as black dots in this figure.

delays [24]. We may, however, reemphasize that any time delay obtained for a finite region via the present method is finite and therefore well-defined, even in the case of the long-range Coulomb potential. As pointed out above, this allows us to study certain aspects with respect to the parameters of the XUV pulse and the effects of an IR streaking in the Coulomb case.

It is necessary to point out that for the Coulomb potential the time delay also depends on the distance that the ionizing wave packet is propagated in the forward direction. This is due to the long-range character of the Coulomb potential since the central momentum of the ionizing wave packet decreases with an increase of the forward propagation distance. Thus, the velocity of the free particle during the backpropagation decreases as well. In Fig. 1(b) we show this effect by presenting results for the time delay from the ground state for two forward propagation distances: $\langle x_{\text{forward}}\rangle = 2000$ (black solid line) and 3000 (blue dashed line). As expected, the time delays for $\langle x_{\text{forward}}\rangle = 3000$ are slightly smaller than those for $\langle x_{\text{forward}}\rangle = 2000$. This shows the need to use rather large grids for the numerical simulations in the case of a Coulomb potential. However, this small dependence on the forward propagation distance does not change our conclusions regarding the convergence of the results towards infinite regions.

We also note from the results in Fig. 1 that the time delay increases most strongly in the region close to the center of the potential, where the potential changes most strongly. This indicates that the results should depend on the choice of the inner boundary x_{inner} of the region R. To study this feature, we fixed the outer boundary of R at $x_{\text{outer}} = 500$, which is large enough to obtain converged results in the case of the Yukawa potential, and then varied the inner boundary x_{inner}. The results in Fig. 2 show the expected dependence on the choice of x_{inner}: The absolute values of the time delays decrease by half as x_{inner} increases from 0 to 5 a.u.. In the remainder of the present studies we have chosen the $x_{\text{inner}} = 0$ a.u. as the inner boundary, since this value corresponds to the expectation value of x for all the bound states investigated here.

C. Wigner-Smith time delay for photoionization in a short-range potential

In the case of the Yukawa potential, we also compared our numerical results, obtained in the time-dependent numerical simulations, with calculations of the WS time delay as a derivative of the induced phase shift, cf. Eq. (4), obtained from a time-independent scattering approach. In order to obtain the latter for photoionization by a light pulse with finite duration, we first considered the scattering of an electron, incident from $x = -\infty$ with a momentum k, of the short-range Yukawa potential. We solved the corresponding time-independent Schrödinger equation numerically using the fourth-order Runge-Kutta method up to $|x| = 500$, projected the numerical solution onto the appropriate plane-wave solutions for $x \to \pm\infty$, and obtained the WS time delay for the scattering process $\Delta t_{\text{WS}}^{(\text{scat})}$ as the derivative of the phase shift in the plane wave propagating in positive x direction with respect to the energy of the incident particle. In order to take account of the energy spread of the ionizing wave packet in a specific photoionization process, we averaged $\Delta t_{\text{WS}}^{(\text{scat})}$ over the energy spectrum of the wave packet, as obtained in our time-dependent numerical simulations. Finally, we considered the photoionization as a half-scattering process and divided the result of the average by two. The resulting WS time delays for photoionization are shown as black dots in Fig. 2 and are in good agreement with our numerical results, obtained from the time-dependent calculations, for $x_{\text{inner}} = 0$ and $x_{\text{outer}} = 500$. This is in support of the applicability of our approach to obtain time delays from the time-dependent numerical simulations.

D. Dependence of time delay on XUV pulse parameters

Next, we studied the dependence of the time delay introduced here on the parameters of the XUV ionizing pulse for photoionization from the ground state of the Yukawa potential. In Fig. 3 we present our results as functions of (a) the XUV frequency at a fixed pulse duration of $\tau = 400$ as and (b) the duration of the XUV pulse at a fixed frequency of $\omega = 100$ eV. The peak intensity was $I = 1 \times 10^{15}$ W/cm^2 and the CEP was $\phi = 0$ in each of these simulations.

The results agree well with qualitative expectations. The absolute value of the time delay decreases towards zero as the frequency of the ionizing XUV pulse and, hence, the final kinetic energy of the emitted electron increases [cf. Fig. 3(a)]. This is due to the fact that the effect of the potential on the motion of the electron becomes negligible in the limit of infinitely large kinetic energy of the electron (i.e., infinite large XUV frequency) and, therefore, the time spent in the potential approaches that of the free particle in this limit.

We further find that the absolute value of the time delay decreases with an increase of the XUV pulse duration [Fig. 3(b)]. This dependence is closely related to that presented in Fig. 3(a) and can be qualitatively understood as follows. Due to the finite pulse duration the ionized electron wave packet has a certain bandwidth about a central kinetic energy. Consequently, the time delay obtained for the wave packet can be considered as an average over contributions at particular electron energies within the bandwidth (weighted by the ionization probability at a given energy). As indicated by the

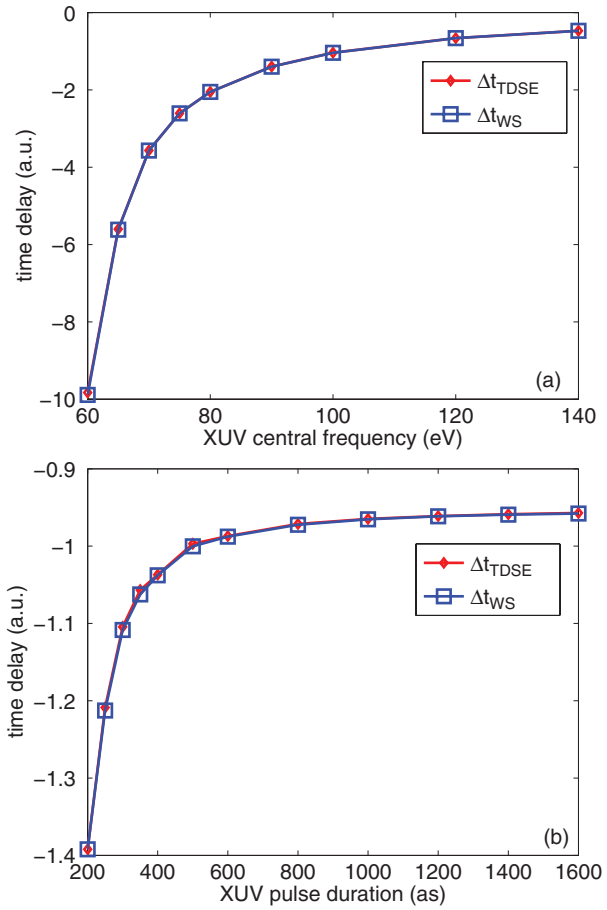

FIG. 3. (Color online) Time delays for ionization from the ground state of the Yukawa potential as functions of (a) the XUV photon frequency ($\tau = 400$ as) and (b) the pulse duration of the XUV pulse ($\omega = 100$ eV). A comparison between results from the present TDSE calculations (red diamonds) and those for the WS time delay (blue open squares) is shown. Other laser parameters were $I = 1 \times 10^{15}$ W/cm^2 and $\phi = 0$.

results in panel (a) the time delay does not change linearly with the kinetic energy. Therefore, the time delay obtained for a wave packet will be smaller than its contribution at the central kinetic energy or the expectation value of the kinetic energy. This difference decreases and, thus, the time delay for the wave packet increases as the energy bandwidth of the wave packet decreases, i.e., as the pulse duration increases. Furthermore, it is found that the expectation value of the kinetic energy of the ionizing wave packet increases as the XUV pulse duration increases, which also causes the time delay to increase.

For each of the results from the time-dependent simulations presented in Fig. 3 we also calculated the WS time delay for photoionization, as described in the previous section. Again, we found excellent agreement between the results from the time-independent scattering approach (blue open squares in Fig. 3) and our numerical time-dependent simulations. We may note parenthetically, that our simulations results also agree well with those of classical calculations (not shown) in which the time delays are determined by

$$\Delta t_{\text{classical}} = \int_0^{x_{\text{outer}}} \frac{1}{\sqrt{2[\langle E\rangle - V(x)]}} dx - \frac{x_{\text{outer}}}{\sqrt{2\langle E\rangle}}, \quad (15)$$

where $\langle E\rangle$ is the expectation value of the kinetic energy E of the electron for a given ionized wave packet.

IV. STREAKING OF PHOTOIONIZATION PROCESSES BY NEAR-INFRARED FIELD

In an attosecond streaking experiment [28], an IR field is used to map time information to the momentum space. One of the questions that arise in this context is whether or not the streaking field influences the observed quantities. Although the time delays introduced here do not necessarily correspond to those observed in recent streaking experiments, we can show, in general, how the effect of the streaking field can be studied with our present method. To this end, we first discuss how the streaking field can be included in the numerical simulations of time delays and then study the impact of a streaking IR field on the time delays for the short-range Yukawa as well as the long-range Coulomb potential by varying the parameters of the streaking field.

A. Streaking field in the numerical simulation

The streaking field is represented by an additional potential V_{streak}, which we consider as part of the potential $V(\boldsymbol{r})$ in Eq. (8). Thus, in the present calculations the streaking field is considered on equal footing with the atomic potential. After (forward) propagation of the wave function from its initial state and separation of the bound and ionizing part of the wave function, we then propagate the ionizing part of the wave function backwards, once within the combination of the atomic potential and the streaking field and once as a free particle.

As a result we obtain the time delay, associated with the ionizing part of the wave function in the combined potential of the short- or long-range interaction and the streaking field as

$$\Delta t^{(\text{IR})}_{\Psi_i,R} = t^{(\text{IR})}_{\Psi_i,R} - t_{\Psi^{(0)},R}, \quad (16)$$

where $t^{(\text{IR})}_{\Psi_i,R}$ is the time the ionizing wave packet spends in region R in the presence of the (short- or long-range) potential and the IR streaking field and $t_{\Psi^{(0)},R}$ is the time for the free particle case.

Here, the forward propagation of the wave function has to be continued as long as the IR streaking field is present. As noted above, for the long-range Coulomb potential the time delay depends on the distance the wave packet is propagated in the forward direction. In order to keep the corresponding error small in our current analysis we used a large grid of $-13\,000$ to $13\,000$ a.u. and stopped the forward propagation when the expectation value of the ionizing wave packet reaches 8000 a.u. We increased the spatial step to $\delta x = 0.1$ and the time step to $\delta t = 0.02$ as compared to the previous calculations. Test calculations showed that the relative error of the present results is about 1%. In order to compare with the results, presented above, we considered the same parameters for the Yukawa and the Coulomb potential as before. We chose the first excited state as the initial state and checked that the ionization induced by the IR field is negligible up to a streaking field intensity of 1×10^{13} W/cm^2, which is large enough for the streaking purpose.

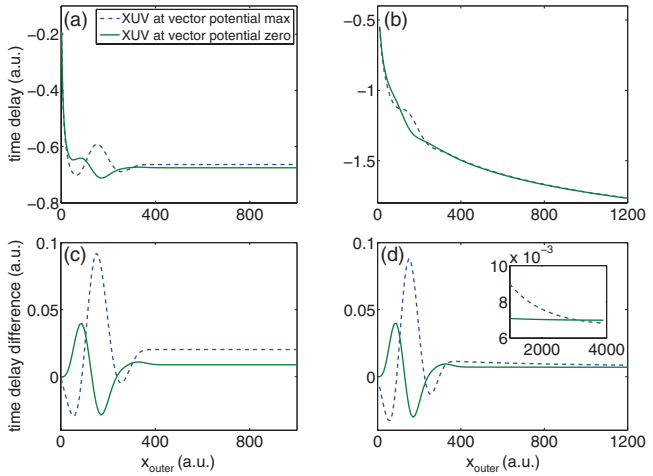

FIG. 4. (Color online) Time delays (top row) and time delay differences (bottom row) as a function of outer boundary x_{outer} of R for Yukawa potential (left column) and Coulomb potential (right column). For each potential we have centered the XUV pulse at two different positions, which correspond to the maximum (blue dash-dotted line) and zero (green solid line) of the IR vector potential, respectively. The XUV parameters are $I_{\text{XUV}} = 1 \times 10^{15}$ W/cm^2, $\omega_{\text{XUV}} = 100$ eV, $\tau_{\text{XUV}} = 400$ as, and $\phi_{\text{XUV}} = 0$. The IR parameters are $I_{\text{IR}} = 1 \times 10^{12}$ W/cm^2, $\lambda_{\text{IR}} = 800$ nm, $N_{\text{IR}} = 3$ cycle, and $\phi_{\text{IR}} = 0$. The small box in (d) shows the long-range behavior of the two curves.

B. Effects of the probing pulse on time delays

In order to analyze the effect of the IR probing field we obtained the time delay for photoionization from the first excited state of the Yukawa as well as the Coulomb potential in the streaking field. To this end, we applied the ionizing XUV pulse centered at the maximum of the IR streaking field (zero of the vector potential) as well as centered at the central zero of the IR streaking field (maximum of the vector potential). In the upper row of Fig. 4 the results for the time delays in the streaking field (green solid lines, XUV centered at zero of the vector potential; blue dashed lines, XUV centered at maximum of vector potential) are shown as a function of the outer boundary x_{outer} of the region R for the Yukawa (left) and the Coulomb potential (right). As in the results without streaking field, we see that there is a well-defined limit of the time delays for the short-ranged Yukawa potential as the region R increases, while there is no convergence found for the Coulomb potential.

In order to see the effect of the probing field, we present in the lower row of Fig. 4 the difference between the time delays in the streaking field and those without streaking field as a function of the outer boundary of the region R, i.e.,

$$\Delta T = \Delta t^{(\text{IR})}_{\Psi_i,R} - \Delta t_{\Psi_i,R}. \tag{17}$$

Although there is no well-defined limit of the time delays for infinite regions in the Coulomb case, neither with nor without streaking field, for any finite region the time delays introduced here are well-defined and the effect of the streaking field can be analyzed. The same argument applies to the weak dependence of the Coulomb results on the distance of forward propagation in our simulations.

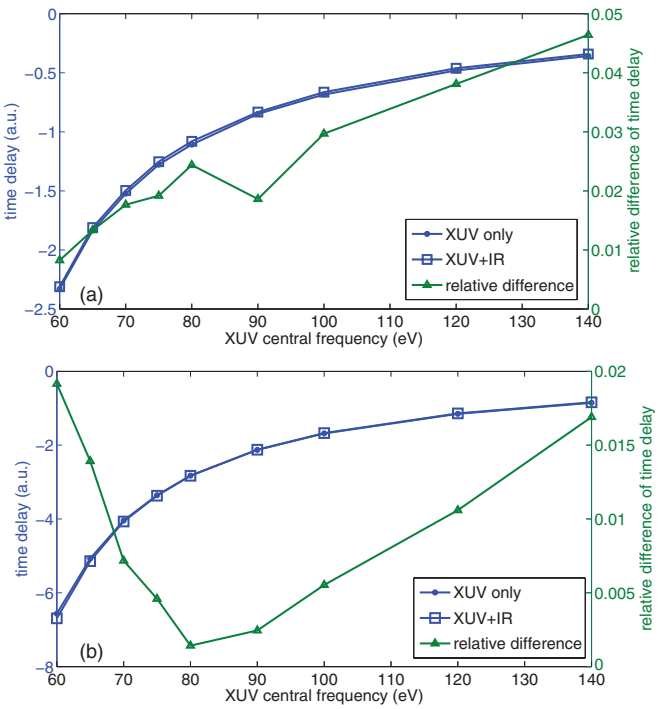

FIG. 5. (Color online) Time delays with (blue open squares) and without (blue solid circles) IR streaking field as well as relative differences between the results (green solid triangles) as a function of XUV central frequency for (a) Yukawa potential and (b) Coulomb potential. The XUV pulse was centered at the middle (maximum vector potential) of the IR field. Other laser parameters are the same as in Fig. 4. For the Coulomb case the time delays are calculated at $x_{\text{outer}} = 800$.

For both potentials, we see that the time-delay difference ΔT oscillates for $x_{\text{outer}} < 400$. This oscillation is due to the presence of the IR field, since the ionized wave packet propagated up to about $x \simeq 400$ before the IR streaking field ceased in the present simulations. We note that the differences ΔT are small, less than 3% for the Yukawa potential and less than the numerical error of 1% for the Coulomb potential, compared to the time delays induced by the atomic potentials themselves. In the present calculations we therefore do not find a significant effect of the streaking field, neither for a short-range nor for a long-range potential.

Before we continue to study further the influence of the IR streaking field, we note a subtle point in the results obtained for the Coulomb potential, which are presented in Fig. 4. While neither the time delays with and without streaking field converge as a function of the outer boundary x_{outer}, we find a converged result (within the numerical error) for the time-delay difference ΔT if the XUV pulse is centered about the zero of the vector potential of the streaking field [see green solid line in Fig. 4(d)]. This occurs since in this case the momentum distribution of the ionizing wave packet at the end of the forward propagation is the same as that of the no-streaking-field case. In contrast, if the XUV pulse is applied at the maximum of the vector potential of the streaking field, the final momentum distribution is shifted and thus no convergence of the time delay difference within the range of

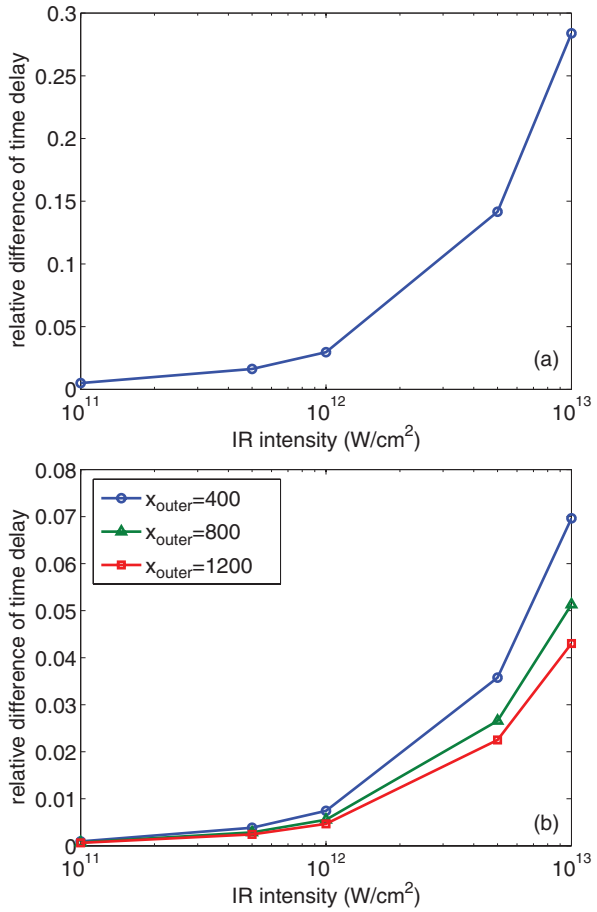

FIG. 6. (Color online) Relative differences of time delay as function of IR intensity for (a) Yukawa potential and (b) Coulomb potential. The XUV pulse is centered at the middle of the IR field. Laser parameters are the same as in Fig. 4 except I_{IR} is changing. For the Coulomb case the time delays are taken at $x_{outer} = 400$, 800, and 1200.

present boundaries is found [see blue dashed line in the inset of Fig. 4(d)].

The conclusion that the streaking field does not influence the time delay introduced here significantly holds over a large range of XUV frequencies as well as for intensities of the streaking field up to about 10^{13} W/cm^2. In Fig. 5 we present the results for the time delay obtained in (a) the Yukawa potential and (b) the Coulomb potential with (blue open squares) and without (blue solid circles) streaking field as a function of the XUV frequency. Since the results are in close agreement we also show the relative difference between them (green solid triangles), which does not exceed 5% and 2% in the Yukawa and Coulomb case, respectively.

As one would expect, the relative difference between the results for the time delay obtained with and without streaking field do increase with an increase of the IR streaking field intensity. This can be clearly seen from the results shown in Fig. 6. It appears that for IR intensities up to 10^{12} W/cm^2 the relative difference between the results is small enough that there is no significant effect on the time delay. While the relative difference quickly increases beyond 10% in the case of the Yukawa potential with a further increase of the IR intensity, the 10% limit is not reached for an IR intensity of 10^{13} W/cm^2 in the case of the Coulomb potential.

V. CONCLUSION

In summary, we have applied a fundamental definition of time delay to time-dependent numerical simulations on the grid. To this end, we have obtained the difference between the time a particle spends in a finite region of a potential and the time a free particle spends in the same region using a backpropagation technique. Our method expands the options for a theoretical analysis of ultrashort time-dependent processes. For any finite region in space the time delay introduced here is well-defined, even for long-range potentials, and time delays can be determined as a function of time after the emission of the photoelectron. The method is applied to photoionization of an electron in a short-range Yukawa as well as a long-range Coulomb potential by an attosecond XUV pulse. It is found that the numerical results are in excellent agreement with those for the (asymptotic) WS time delay, obtained as the derivative of the phase shift with respect to the energy, for the short-range potential. In contrast, the numerical results in the case of the Coulomb potential are finite for any finite region, but they do not converge as the region increases to infinity, as expected. The well-defined time delays for a finite region enabled us to study the impact of a near-IR streaking (or probing) pulse for both potentials. For the time delays introduced in this paper, our results show that the effect is small as long as the intensity of the probing field is below 10^{13} W/cm^2.

ACKNOWLEDGMENTS

J.S. and A.B. acknowledge financial support by the US Department of Energy, Division of Chemical Sciences, Atomic, Molecular, and Optical Sciences Program. H.N. was supported via a grant from the US National Science Foundation (Award No. PHY-0854918). A.J.-B. acknowledges financial support by the US National Science Fundation (Award No. PHY-1068706). This work utilized the Janus supercomputer, which is supported by the US National Science Foundation (Award No. CNS-0821794) and the University of Colorado Boulder. The Janus supercomputer is a joint effort of the University of Colorado Boulder, the University of Colorado Denver, and the National Center for Atmospheric Research.

[1] M. Drescher, M. Hentschel, R. Kienberger, M. Uiberacker, V. Yakovlev, A. Scrinzi, T. Westerwalbesloh, U. Kleineberg, U. Heinzmann, and F. Krausz, Nature (London) **419**, 803 (2002).

[2] E. Goulielmakis, Z.-H. Loh, A. Wirth, R. Santra, N. Rohringer, V. S. Yakovlev, S. Zherebtsov, T. Pfeifer, A. M. Azzeer, M. F. Kling, S. R. Leone, and F. Krausz, Nature (London) **466**, 739 (2010).

[3] M. Uiberacker, T. Uphues, M. Schultze, A. J. Verhoef, V. Yakovlev, M. F. Kling, J. Rauschenberger, N. M. Kabachnik, H. Schrder, M. Lezius, K. L. Kompa, H. G. Muller, M. J. J. Vrakking, S. Hendel, U. Kleineberg, U. Heinzmann, M. Drescher, and F. Krausz, Nature (London) **446**, 627 (2007).

[4] E. Gagnon, P. Ranitovic, X.-M. Tong, C. L. Cocke, M. M. Murnane, H. C. Kapteyn, and A. S. Sandhu, Science **317**, 1374 (2007).

[5] A. L. Cavalieri, N. Müller, T. Uphues, V. S. Yakovlev, A. Baltuška, B. Horvath, B. Schmidt, L. Blümel, R. Holzwarth, S. Hendel, M. Drescher, U. Kleineberg, P. M. Echenique, R. Kienberger, F. Krausz, and U. Heinzmann, Nature (London) **449**, 1029 (2007).

[6] M. Schultze *et al.*, Science **328**, 1658 (2010).

[7] K. Klünder, J. M. Dahlström, M. Gisselbrecht, T. Fordell, M. Swoboda, D. Guénot, P. Johnsson, J. Caillat, J. Mauritsson, A. Maquet, R. Taïeb, and A. L'Huillier, Phys. Rev. Lett. **106**, 143002 (2011).

[8] A. S. Kheifets and I. A. Ivanov, Phys. Rev. Lett. **105**, 233002 (2010).

[9] C.-H. Zhang and U. Thumm, Phys. Rev. A **82**, 043405 (2010).

[10] S. Nagele, R. Pazourek, J. Feist, K. Doblhoff-Dier, C. Lemell, K. Tökési, and J. Burgdörfer, J. Phys. B **44**, 081001 (2011).

[11] M. Ivanov and O. Smirnova, Phys. Rev. Lett. **107**, 213605 (2011).

[12] L. R. Moore, M. A. Lysaght, J. S. Parker, H. W. van der Hart, and K. T. Taylor, Phys. Rev. A **84**, 061404 (2011).

[13] C.-H. Zhang and U. Thumm, Phys. Rev. A **84**, 033401 (2011).

[14] A. S. Kheifets, I. A. Ivanov, and I. Bray, J. Phys. B **44**, 101003 (2011).

[15] I. A. Ivanov, Phys. Rev. A **83**, 023421 (2011).

[16] I. A. Ivanov, Phys. Rev. A **86**, 023419 (2012).

[17] S. Sukiasyan, K. L. Ishikawa, and M. Ivanov, Phys. Rev. A **86**, 033423 (2012).

[18] J. M. Dahlström, A. L'Huillier, and A. Maquet, J. Phys. B **45**, 183001 (2012).

[19] M. D. Spiewanowski and L. B. Madsen, Phys. Rev. A **86**, 045401 (2012).

[20] D. Guénot, K. Klünder, C. L. Arnold, D. Kroon, J. M. Dahlström, M. Miranda, T. Fordell, M. Gisselbrecht, P. Johnsson, J. Mauritsson, E. Lindroth, A. Maquet, R. Taïeb, A. L'Huillier, and A. S. Kheifets, Phys. Rev. A **85**, 053424 (2012).

[21] R. Pazourek, J. Feist, S. Nagele, and J. Burgdörfer, Phys. Rev. Lett. **108**, 163001 (2012).

[22] S. Nagele, R. Pazourek, J. Feist, and J. Burgdörfer, Phys. Rev. A **85**, 033401 (2012).

[23] E. P. Wigner, Phys. Rev. **98**, 145 (1955).

[24] F. T. Smith, Phys. Rev. **118**, 349 (1960).

[25] R. G. Newton, *Scattering Theory of Waves and Particles* (Springer-Verlag, New York, 1982), Chap. 11.

[26] Y. K. Ho, Phys. Rep. **99**, 1 (1983).

[27] C. W. McCurdy, M. Baertschy, and T. N. Rescigno, J. Phys. B **37**, R137 (2004).

[28] J. Itatani, F. Quéré, G. L. Yudin, M. Y. Ivanov, F. Krausz, and P. B. Corkum, Phys. Rev. Lett. **88**, 173903 (2002).